Journal of Solid State Chemistry **167,** 126–136 (2002)
doi:10.1006/jssc.2002.9634

Structural Investigations of $ACu_3Ru_4O_{12}$ (A=Na, Ca, Sr, La, Nd)—A Comparison between XRD-Rietveld and EXAFS Results

S. G. Ebbinghaus,*,[1] A. Weidenkaff,* and R. J. Cava†

*Institut für Physik, Universität Augsburg, Universitätsstraße 1, D-86159 Augsburg, Germany; and †Department of Chemistry, Princeton University, Princeton, New Jersey 8544

The structures of five perovskite-related oxides with the general composition $ACu_3Ru_4O_{12}$ with A = Na, Ca, Sr, La and Nd, have been examined both by XRD-Rietveld refinements and Ru-K EXAFS-spectroscopy. In addition, the behavior on reduction was investigated by thermogravimetry (TG). The TG measurements revealed that the composition was almost exactly $A_1Cu_3Ru_4O_{12}$ for all samples. The inter-atomic distances derived from EXAFS- and XRD-Rietveld fits show an excellent agreement with differences smaller than 8 mÅ even for $R > 5$ Å. All inter-atomic distances increase in the order Na < Ca < Sr < Nd < La and were found to depend linearly on the product of charge and ionic radius of the A-cation. The experimentally found distances are compared with the corresponding values expected from bond-valence calculations.

Key Words: **EXAFS; Rietveld structure refinements; perovskites; cuprates; ruthenates.**

INTRODUCTION

The determination of crystal structures of polycrystalline compounds by XRD-Rietveld refinement calculations is a well-established and widely used procedure (1).

Although this method has been successfully applied in hundreds of cases, it has some disadvantages. One of its problems is that due to their large scattering factors, the peak intensities of XRD patterns are dominated by heavy atoms like Ba, La, Bi, etc. while elements with lower atomic number (like oxygen) contribute little to the peak intensities. As a consequence, the atomic positions of these elements cannot often be determined very precisely. For many perovskite-related compounds, on the other hand, the positions of the oxygen ions are of great interest, because structural modifications are often accompanied by tiltings or rotations of the metal-oxygen-polyhedra. One nice example is Sr_2IrO_4, which differs from its higher symmetry Sr_2RuO_4 analogue only by a slight rotation of the IrO_6-octahedra (2, 3).

While a precise determination of oxygen positions can be achieved by using neutrons instead of X rays, a more serious problem remains: All diffraction methods rely on well-crystallized samples with a sufficiently large grain size. In recent years, new preparation techniques like co-precipitation, sol–gel synthesis or microemulsion methods have widely been applied. Their advantage is that the reactants are already mixed on an atomic scale before calcination and therefore react more easily and/or at lower temperatures. In addition, the reaction products often differ from the ones achieved by classical solid-state reactions, e.g., metastable phases can be prepared. The products resulting from these preparation techniques often show broad diffraction peaks due to poor crystallinity and/or small particle sizes and, therefore, they are not suitable for Rietveld calculations. Also the increasing interest in nano- or meso-structured materials requires new characterization techniques other than diffraction methods because these compounds generally exhibit very broad peaks or they are even X-ray-amorphous though they might possess a high degree of short-range ordering.

With the development of modern synchrotron radiation sources, Extended X-ray Absorption Fine Structure (EXAFS) spectroscopy has become a popular tool for the determination of inter-atomic distances and coordination numbers. In contrast to diffraction methods, EXAFS can be used for amorphous, liquid, or gaseous samples as well. The two methods complement each other, as diffraction techniques give information about long-range ordering while EXAFS is a local probe, which yields information about the neighbors within a sphere of a few angstroms around the absorbing atom.

The accuracy of distances and coordination numbers derived from EXAFS investigations depends strongly on the quality of the backscattering phases and amplitudes used in the fitting procedure. These phases and amplitudes are either derived from well-defined reference compounds or they are calculated theoretically. The distances calcu-

[1] To whom correspondence should be addressed. Fax: ++49-821-598-3002. E-mail: stefan.ebbinghaus@physik.uni-augsburg.de.

0022-4596/02 $35.00

lated from EXAFS data are generally believed to possess an error of approximately ± 0.02 Å (4), whereas in the case of X-ray diffraction the inter-atomic distances can be achieved with an accuracy of a few mÅ. For this reason, it is interesting to compare both methods in order to see what kind of agreement can actually be achieved. These results can provide useful additional information for the interpretation of measurements on nano- or mesoscopic or amorphous samples.

A good agreement can also be considered as a verification of the correctness of the backscattering phases and amplitudes used, whereas larger differences indicate that these values need to be modified. This is especially interesting if phases and amplitudes calculated from first principles have been used in the comparison.

In a previous paper a comparison between Ru-K EXAFS and XRD measurements has been described for the system $La_{2-x}Sr_xCu_{1-y}Ru_yO_{4-\delta}$ (5). Unfortunately, the compounds of this system possess a rather complex structure: Derived from the K_2NiF_4-structure type, data analysis is complicated by the fact that La/Sr and Cu/Ru share the *A*- and *B*-type cationic positions. In addition, in these materials the Ru–O distances for the equatorial and axial oxygen atoms differ significantly.

The compounds studied in this work have a higher symmetry structure with only one atomic species per crystallographic site and are therefore much better suited for a comparison between the two experimental methods. The structure of $A Cu_3Ru_4O_{12}$ can be considered as a $2 \times 2 \times 2$ superstructure of the simple cubic perovskite ABO_3 in which the *A*- and Cu-ions share the *A*-position of the perovskite. Thus the composition can be described as $4^*((A_{1/4},Cu_{3/4})RuO_3$. The ruthenium ions are located at $(\frac{1}{4}, \frac{1}{4}, \frac{1}{4})$ while the oxygen ions are shifted from $(\frac{1}{4}, \frac{1}{4}, 0)$ to roughly (0.18, 0.31, 0) (6). This dislocation changes the coordination geometry for $\frac{1}{4}$ of the *A*-cations from a cuboctahedron (in the simple perovskite) to an icosahedron. At the same time the cuboctahedra of the remaining $\frac{3}{4}$ of the *A*-type ions become strongly distorted. In the ideal cubic perovskite all 12 metal-oxygen distances are approximately 2.6 Å. In $A Cu_3Ru_4O_{12}$, on the other hand, four distances are reduced to approximately 2 Å, while the other distances are elongated to 4×2.8 Å, and 4×3.3 Å, respectively. Therefore, the coordination sphere can be considered as a square plane to a first approximation. Such an environment provides the ideal geometry for Jahn–Teller active ions like Cu^{2+}. As a consequence, copper—otherwise a typical *B*-type cation—occupies an *A*-position with respect to the usual nomenclature ABO_3. Fig. 1 shows a presentation of the crystal structure in which the RuO_6-octahedra and the CuO_4-squares can well be seen.

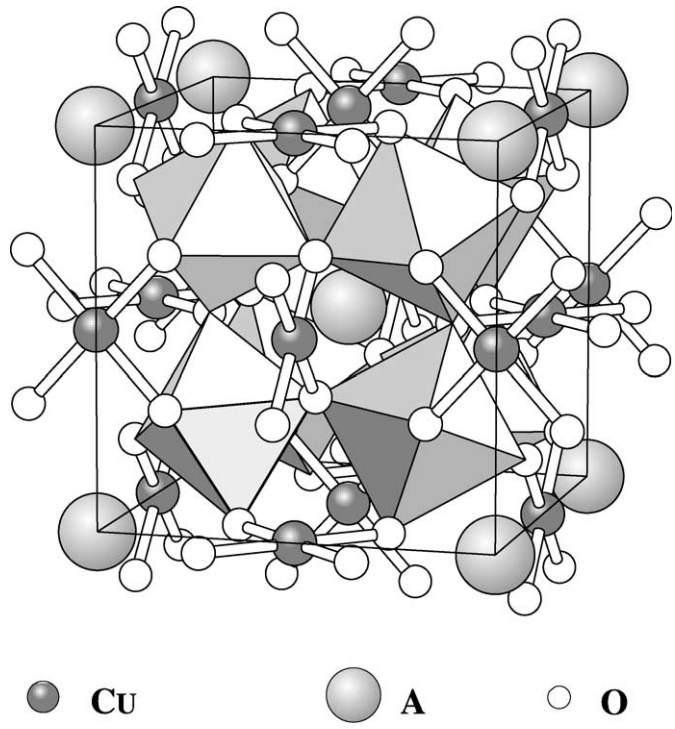

FIG. 1. Crystal structure of $A Cu_3Ru_4O_{12}$. The octahedra represent RuO_6-units.

EXPERIMENTAL

The polycrystalline samples were prepared by conventional solid-state reactions, starting from well-ground mixtures of RuO_2, CuO and Na_2CO_3, $CaCO_3$, $SrCO_3$, La_2O_3 or Nd_2O_3. The mixtures were heated in alumina crucibles at 1050°C for 48 h. To achieve single-phase products, we found it necessary to use a small excess of CuO, which was dissolved in diluted HCl (approximately 1 N) after the reaction.

Thermogravimetric measurements were performed on a Netzsch 409 thermobalance connected to a Balzers QMG quadrupole mass spectrometer by a skimmer coupling system. About 100 mg of the oxides were heated in flowing forming gas (10% H_2 in N_2; 50 mL/min) to 1250°C with a heating rate of 10°C/min and kept at this temperature for 30 min.

EXAFS measurements were performed at the beamline X1.1 of HASYLAB at DESY. The beam was monochromatized with a Si-(3 1 1) double-crystal monochromator. About 50 mg of the oxides and 20 mg of polyethylene were thoroughly mixed and pressed in to pellets of 13 mm diameter. These were measured in transmission mode at 77 K in the energy range 21,900–23,500 eV. The EXAFS region was measured in equidistant k steps ($\Delta k \approx 0.04$ Å^{-1}) and the counting time was increased linearly with k, starting from 1.5 s/data point and ending at 8.5 s/data

point. The spectra were energy-calibrated against the first inflection point of the K edge spectra of Ru-metal (22.117 keV) which was measured simultaneously.

For data evaluation, the program WinXAS (7) was used. The pre-edge region was fitted with a Victoreen function. This function was then extended over the whole spectrum and subtracted from the data. The spectra were normalized by setting the average absorption coefficient between 22.17 and 22.22 keV to the value of 1. The photon energy (E) to wave vector (k) conversion was carried out using the first inflection point of the absorption edge as the energy threshold. The atomic absorption μ_0 was subtracted by fitting the k^3 weighted spectra in the range $3.95 \leq k \leq 19.5\,\text{Å}^{-1}$ with a seventh-degree polynomial function. Before the Fourier transformation the data were weighted with a Bessel window ($\beta = 4$). Theoretical scattering phase shifts and amplitudes used for the fitting procedure were calculated with the program FEFF6.01 (8).

X-ray diffraction data were collected on a Seifert XRD 3003-TT diffractometer using Cu$K\alpha$ radiation in the angular range $15^\circ \leq 2\theta \leq 150^\circ$. The stepsize was 0.015° 2θ with a counting time of 6 s per data point.

For Rietveld refinement calculations the program Fullprof98 was used (9). The background was approximated by a linear interpolation between approximately 40 data points in regions where no Bragg reflections were present. For the peak shape a pseudo-Voigt profile function was applied.

RESULTS AND DISCUSSION

Thermogravimetry

Thermogravimetric measurements often provide an elegant way to determine the (oxygen-) stoichiometry of transition metal oxides. By heating them in a reducing atmosphere (usually forming gas, i.e., mixtures of H_2 with N_2 or Ar) most perovskites are reduced to the corresponding metals or simple binary oxides. These products can easily be identified by X-ray diffraction. The observed weight loss is then compared with the one expected for the assumed composition. In the case of mixed perovskites, e.g., $AB_{1-x}B'_xO_{3-\delta}$ a good agreement between these two values proves that both x is correct and that δ is zero. Of course, the situation becomes more complicated if the observed weight loss does not exactly match the expected one: This might either be due to an oxygen-nonstoichiometry ($\delta \neq 0$) or due to a value of x other than expected. In this case a second method to determine δ or x is needed. The problem of carbonated samples can easily be overcome by simultaneously measuring the gaseous reduction products with mass spectroscopy. The evolution of CO_2 or other volatile compounds (e.g., NO_x due to incomplete reaction of nitrate precursors) is revealed by characteristic m/e peaks in the mass spectrum.

In our case the reduction of $ACu_3Ru_4O_{12}$ leads to Ru- and Cu-metal and the binary oxides of the A cations. During the reaction no volatile products other than H_2O were detected. Figure 2 depicts the weight loss for the five compounds under investigation. Constant lines represent the expected values calculated for the ideal composition. A very good agreement between observed and expected weight losses was found. In the case of A = Na, three reduction steps were observed. While the first step corresponds well to a formation of Na_2O_2, the second step could be assigned to a complete loss of oxygen, i.e., the reduction to Na-metal ($\Delta m_{\text{obs}} = -23.78\%$, $\Delta m_{\text{calc}} = -23.71\%$). The metallic sodium evaporates at higher temperatures, resulting in a final weight loss of 26.5%.

The numerical results of the TG experiments are listed in Table 1. Minor deviations from the expected values have been expressed in terms of oxygen deficiencies. As can be seen, the maximum δ value is 0.11 (A = Sr), which corresponds to a value of 0.03 with respect to the simple perovskite stoichiometry $ABO_{3-\delta}$. This deviation is well within the accuracy of the method and therefore we conclude that the composition of all five samples must be very close to the ideal stoichiometry $ACu_3Ru_4O_{12}$. This result is not too surprising, because any oxygen deficiency would lead to a destruction of the RuO_6 octahedra, which are known to be very rigid units: In a previous paper it was demonstrated that in the system $La_{2-x}Sr_xCu_{1-y}Ru_yO_{4-\delta}$ the RuO_6 octahedra remain intact even if δ reaches values of 0.3 (5). The observed oxygen vacancies were found to lie exclusively in the Cu environment.

The verification of the assumed composition turned out to be a very important information for the interpretation of

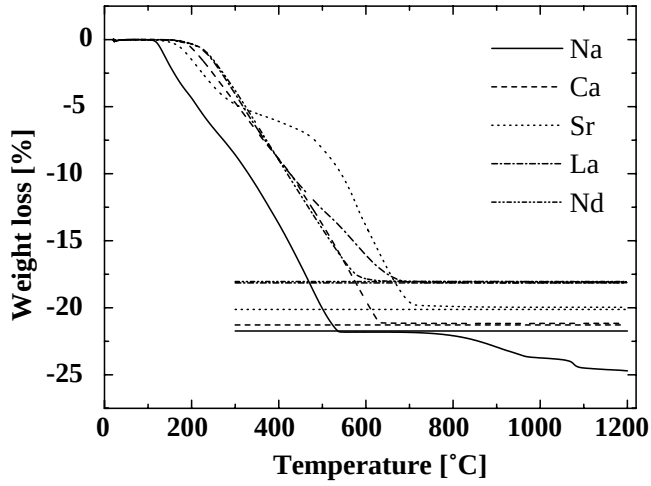

FIG. 2. Relative weight loss during reduction in forming gas.

TABLE 1
Observed (Δm_o) and Calculated Weight Losses (Δm_c) during Reduction in Forming Gas

$A=$	Na	Ca	Sr	La	Nd
Δm_o (%)	−21.81	−21.17	−19.96	−18.14	−18.05
Δm_c (%)	−21.73	−21.28	−20.13	−18.15	−18.04
δ	−0.05	0.07	0.11	0.01	0.00

Note. δ denotes the deviation of the two values expressed in units of oxygen vacancies.

the XRD-Rietveld and EXAFS results as will be discussed in the following.

Ru-K EXAFS

In Fig. 3a, the k^3-weighted $\chi(k)$ of $CaCu_3Ru_4O_{12}$ is shown. As can be seen, the signal-to-noise ratio is very good: even at k-values of 20 $Å^{-1}$, clear EXAFS oscillations are observed. The Fourier transformation leads to sharp and well-separated peaks up to $R \approx 7$ Å, as depicted in Fig. 3b. To assign these peaks to the different coordination shells, theoretical phases and amplitudes were calculated.

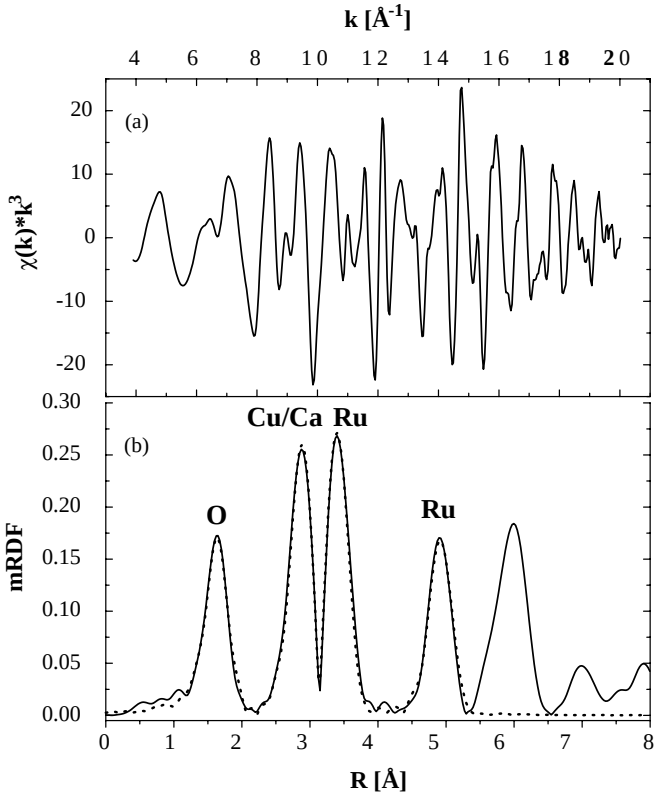

FIG. 3. (a): k^3-weighted EXAFS-function $\chi(k)$ for $CaCu_3Ru_4O_{12}$. (b): The corresponding Fourier transform (solid line) and its fit (dotted line).

The keep criteria for plane and curved wave amplitude filters were set to 5% and 8%, respectively. As the starting structural model, the refined cell parameters derived from the XRD measurements (see below) and the fractional atomic coordinates given by Muller *et al.* for $NdCu_3Ru_4O_{12}$ (10) were used. The relevance of the different scattering paths was then checked by calculating their contribution to the mRDF. While the first peak in the mRDF was assigned to the six oxygen atoms of the RuO_6-unit, the second peak is a superposition of the backscattering of the A- and Cu-cations (both with a distance of $\sqrt{3}/4 \cdot \mathbf{a}$). The contribution of the next nearest oxygen neighbors at a distance of ≈ 3.7 Å was found to be very small so this path could be neglected. For the nearest Ru-neighbor (Ru(nn)), two possible scattering paths have to be considered, namely the direct Ru–Ru scattering and a multiple-scattering path involving the bridging oxygen ion. By comparing the amplitudes and phases of both paths we found that the direct scattering is by far the more important process. This is in contrast to the system $La_{2-x}Sr_xCu_{1-y}Ru_yO_{4-\delta}$ in which the multiple scattering was found to dominate (5). This can be explained by the different Ru–O–Ru bond angle in both types of compounds: While it is exactly 180° in $La_{2-x}Sr_xCu_{1-y}Ru_yO_{4-\delta}$, the angle is reduced to approximately 140° in $ACu_3Ru_4O_{12}$ (10). It is well known that multiple scattering paths play an important role for co-linear arrangements while their amplitude decreases dramatically with a decrease of the angle (11).

The peak at $R \approx 5$ Å was assigned to a single backscattering process from the next-nearest Ru neighbor located at a distance of $\sqrt{2}/2 \cdot \mathbf{a}$.

While all peaks within a sphere of 5 Å are caused by one or two dominating backscattering paths, the peaks at higher distances are not that simple to explain. Considering the various possibilities, we found that a number of scattering processes (including several multiple scattering paths) contribute to these peaks with comparable amplitudes. For this reason a meaningful analysis of these high-distance peaks is not possible and we have restricted our further evaluations to the four peaks mentioned above. Figure 4 shows a graphical presentation of the different paths used in the fits.

The fitting procedure was similar to the one described in (5): As S_0^2, σ, and N are highly correlated (12) their simultaneous refinement might lead to ambiguous values. Therefore, in a first step we have fixed the coordination numbers for one arbitrarily chosen compound ($CaCu_3Ru_4O_{12}$) and refined only the distances, S_0^2, E_0 and the Debye–Waller factors. In a second step we then fixed S_0^2 for the other samples, and refined R, N and σ for all atoms together with the global parameter E_0. For the Cu/A-shell, we used the restriction $N(A) + N(\mathrm{Cu}) = 8$. It soon turned out that the so-obtained values for the Debye–Waller

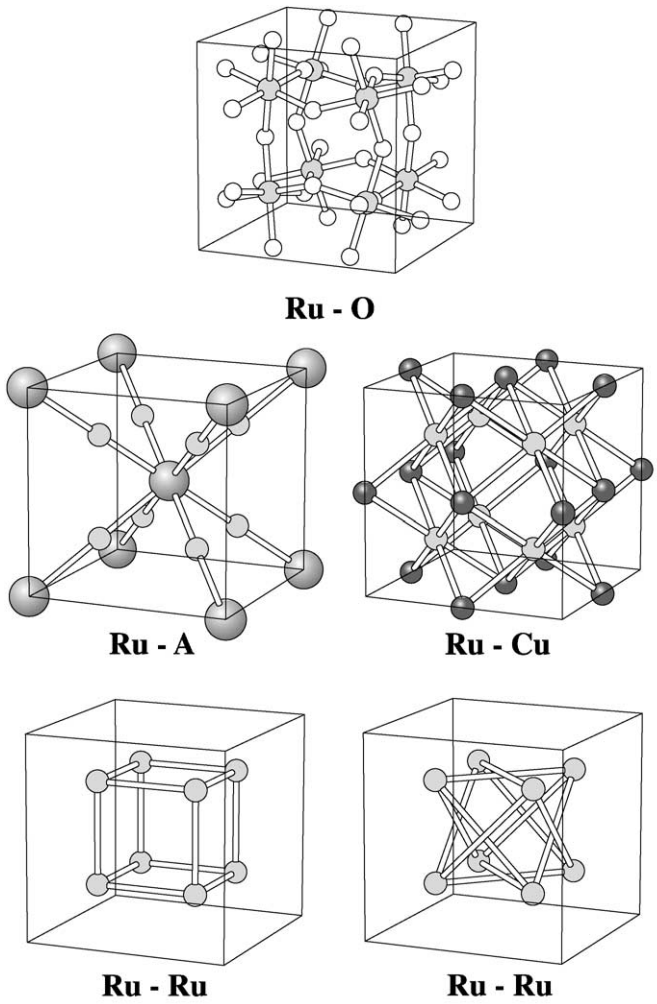

FIG. 4. Main EXAFS backscattering paths.

factors were almost identical for all compounds. Therefore, we decided to use the same averaged σ-values for each atomic species in all refinements. Figure 3b depicts a typical fit result. Evidently, the experimental data can be reproduced well by the fit. Table 2 lists the numerical values for the coordination number and distances obtained. As can be seen, the coordination numbers agree very well with the expected values. For the oxygen shell the largest deviation is only 0.2 for $A = \mathrm{Nd}$ which means a relative error of 3%. For the other shells the largest differences were found in the case of $A = \mathrm{La}$. The maximum absolute error was $\Delta N = -1$ for the second Ru-shell of this compound. But even this corresponds to a relative error of only -8%. Changing the values for the Debye–Waller factors of La, Ru(nn), and Ru(nnn) to 0.00185, 0.00168, and 0.00252 $\mathrm{\AA}^2$, respectively, led to correct coordination numbers, i.e., 2.08(8), 5.95(6), and 11.92(15). It is not yet clear whether these slightly different Debye–Waller factors for $LaCu_3Ru_4O_{12}$ are due to a larger (static or dynamic) disorder or simply an artifact.

Temperature factors from EXAFS and diffraction methods have a different physical meaning and can not therefore be compared directly (13). Nevertheless, it is interesting to consider the values: If the Debye–Waller factors given in Table 2 are multiplied by $8\pi^2$ to bring them to the same scale as B_{iso}, values of 0.10, 0.15, 0.11, 0.12, and 0.18 $\mathrm{\AA}^2$ are obtained for O, Cu, *A*, Ru(nn), and Ru(nnn), respectively. Although these values are smaller than what would be expected for X-ray diffraction experiments (roughly 0.5 and 0.8 $\mathrm{\AA}^2$ for heavy atoms and oxygen, respectively), they have the correct order of magnitude. Differences result from the fact that our EXAFS measurements were performed at 77 K and that EXAFS only detects the component of the relative displacement which lies along the equilibrium bond direction.

The distances derived from the EXAFS-fits are discussed in the next section in comparison to the XRD-Rietveld results. Here, we only mention that all distances increase with the charge of the *A*-cation. For those compounds with equally charged *A*-cations (e.g., Ca^{2+} and Sr^{2+}), the distance increases with the ionic radius of *A* (14). Apparently, the distances are affected both by steric and electronic factors. Figure 5 shows a plot of the various distances as a function of charge$*$ionic radius. As can be seen, all distances follow the same almost perfectly linear relation with the order of bond distances being $\mathrm{Na} < \mathrm{Ca} < \mathrm{Sr} < \mathrm{Nd} < \mathrm{La}$.

This kind of relationship is quite unusual and has not been reported before to the best of our knowledge. It reflects both the steric effects of the *A*-cation and the shrinking of the ruthenium ions with increasing oxidation state (a higher charge of the *A*-cation leads to a lower oxidation state for Ru). However, attempts to directly correlate the observed behavior to the ruthenium oxidation state were not quite satisfactory: Plots of the distances vs the ratio (*A*-cation size)/(Ru charge) or vs the product (*A*-cation size)$*$(Ru charge) did not reveal a linear behavior.

During the EXAFS fits, the distances Ru–A/Cu, Ru–Ru(nn) and Ru–Ru(nnn) were refined independently although actually they are linked due to the crystallographic symmetry: As the fractional coordinates are (0,0,0), ($\frac{1}{2}$, 0, 0), and ($\frac{1}{4}$, $\frac{1}{4}$, $\frac{1}{4}$) for *A*, Cu and Ru, respectively, the ratio of the above-mentioned distances is 0.8660:1:1.4142. Calculating the distance ratios for the various compounds revealed a surprisingly good agreement between observed and theoretical values: For example a ratio of 0.8642:1:1.4134 was found for $NaCu_3Ru_4O_{12}$. The highest deviation observed was less than 2.5‰ ($A = \mathrm{Sr}$, Ru–*A*/Ru–Ru(nn))! This excellent agreement is a proof of the high accuracy of the distances achieved by EXAFS analysis.

TABLE 2
Refined Structural Parameters for the Ru–K EXAFS Analysis of $ACu_3Ru_4O_{12}$

			Atom		O	Cu	*A*	Ru	Ru
				σ ($\times 10^{-3}$ Å^2)	1.31	1.85	1.45	1.58	2.29
$S_0^2 = 0.72$		R (%)[a]	E_0 (eV)						
A =	Na	6.94	−3.45(5)	*N*	5.98(3)	5.97(2)	2.03(2)	5.97(2)	11.99(5)
				R (Å)	1.9706(3)	3.1930(2)	3.1930(2)	3.6949(2)	5.2223(3)
	Ca	6.12	−2.66(6)	*N*	5.93(3)	5.98(2)	2.02(2)	6.00(2)	12.17(6)
				R (Å)	1.9787(4)	3.2137(3)	3.2137(3)	3.7120(3)	5.2463(4)
	Sr	6.98	−4.70(8)	*N*	6.02(4)	6.05(3)	1.95(3)	6.01(2)	12.09(8)
				R (Å)	1.9851(5)	3.2193(6)	3.2193(6)	3.7266(3)	5.2665(5)
	La	6.31	−2.34(13)	*N*	6.13(7)	6.46(3)	1.54(3)	5.72(2)	11.0(1)
				R (Å)	1.9941(9)	3.2363(5)	3.2363(5)	3.7432(6)	5.2898(9)
	Nd	6.03	−3.47(15)	*N*	6.21(8)	6.02(6)	1.98(6)	6.04(5)	12.08(17)
				R (Å)	1.9887(9)	3.2300(5)	3.2300(5)	3.7330(7)	5.2735(11)

[a] $R = \frac{\sum_{i=1}^{N} |y_{exp}(i) - y_{theo}(i)|}{\sum_{i=1}^{N} |y_{exp}(i)|} \cdot 100.$

XRD-Rietveld

Although the crystal structure of the title compounds is rather simple, the Rietveld refinement calculations were not as straightforward as expected. As most of the atoms are occupying special positions, only *x* and *y* of the oxygen ions and the displacement parameters need to be refined.

The displacement parameter for Cu was found to be almost identical within all samples. The *B* values for Ru and O, on the other hand, showed strong deviations for the various compounds and were smaller than expected. For the *A*-cations reasonable *B* values were found for La, Nd and Sr, while extremely large values were observed for Ca and Na, respectively. Large displacement parameters are usually a hint for vacancies on the corresponding crystallographic site. Allowing the occupation factor to vary led to values of 75% for Ca and 43% for Na. Our thermogravimetric measurements, on the other hand, proved that the composition must be very close to the idealized stoichiometry $ACu_3Ru_4O_{12}$ and therefore no *A*-cation vacancies can be present in the samples. Another possible explanation for the very large *B* values is a disorder of Na and Ca, i.e., the *A*-cations are not positioned exactly on (0,0,0). From our EXAFS results we can exclude this possibility, too: *A* (static or dynamic) disorder leads to a strong decrease and broadening of the corresponding peak in the mRDF. As the Debye–Waller factors were fixed in our refinements, this hypothetical disorder would have led to a very small coordination number of the *A*-cations, which we did not observe (see

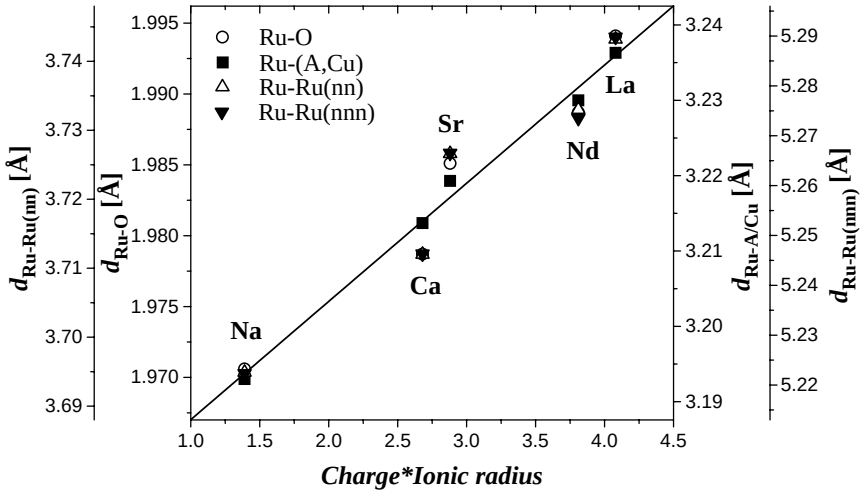

FIG. 5. Inter-atomic distances derived from the EXAFS-fits as a function of (charge∗ionic radius) of the *A* cation. The esds for the distance Ru–O are approximately twice the size of the symbol, for the other distances they are well below the size of the symbols.

Table 2). For these reasons, we believe that the large displacement parameters observed in the Rietveld refinement are simply an artifact (perhaps due to microabsorption or high surface roughnesses). To avoid this problem, we have correlated the B values of Na and Ca with the displacement parameters of the Cu-ions: For A = Nd, La and Sr, the ratio of B_{Cu}/B_A was found to be approximately 0.6:0.4. Our EXAFS results have shown that the Debye–Waller factors for the different atom species must be very similar for all samples. For this reason, we fixed the above-mentioned ratio for A = Ca and Na, respectively. This procedure led to higher R values but to reasonable displacement parameters. Table 3 summarizes the final results of our refinement calculations. As can be seen, satisfactory small R values were achieved for all samples. The largest values (for A = Nd) were $R_p = 7.69\%$ and $R_{wp} = 9.89\%$. The Rietveld plot for this compound is shown in Fig. 6.

Often, χ^2 ($=(R_{wp}/R_{exp})^2$) is a more reliable measure for the quality of a Rietveld refinement. With χ^2 values of approximately 1.4 the structure refinements can be considered to be very good. In Table 4 the inter-atomic distances are listed. Figure 7 shows a plot of these distances as a function of the product (charge∗ionic radius) of the A-cation. Only d_{Ru-O} and **a** are given, because most of the bond lengths are completely determined by the cell parameter. As can be seen, exactly the same behavior as described for the EXAFS-distances (Fig. 5) is observed.

It would be interesting to compare our results with data given in the literature. Unfortunately, only little information can be found for $ACu_3Ru_4O_{12}$. Muller *et al.* have published the single crystal X-ray data for A = Nd (10). In the same paper distances for A = Ca are also listed, yet further information is missing. Our Ru–O distances agree well with those reported (1.982 and 1.986 Å for A = Ca and Nd, respectively). The distances Cu–O (1.933 and 1.930 Å) are only slightly smaller than the ones we found. Furthermore, our Cu–O distances are comparable to the values for other related compounds, namely $CaCu_3Ti_4O_{12}$ (1.961 Å) (15), $CaCu_3Ge_4O_{12}$ (1.960 Å) (16), $Tb_{2/3}Cu_3Ti_4O_{12}$ (1.969 Å) (15), or $NdCu_3Ti_3FeO_{12}$ (1.982 Å) (10). Finally, our cell parameters are in accordance with the values previously given by Labeau *et al.* (17). All these agreements can be considered as a good confirmation of our results.

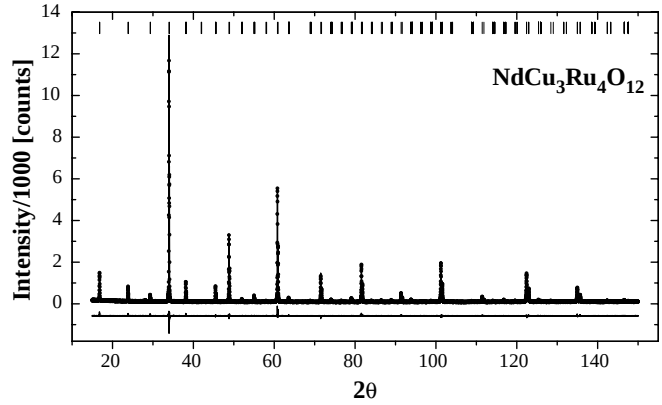

FIG. 6. Rietveld refinement plot for $NdCu_3Ru_4O_{12}$.

A comparison of the distances derived from EXAFS- and XRD-fits (Table 4 and Fig. 8) reveals an excellent agreement. The deviations are smaller than ± 0.008 Å for all coordination shells up to $R > 5$ Å. The differences for the oxygen shell range from -0.002 Å for Ca to $+0.007$ Å for Na, respectively. For the A/Cu-shell the d_{EXAFS}-$d_{Rietveld}$ ranges from -0.006 Å (Sr) to $+0.001$ Å (Ca). For the two Ru-spheres the differences are almost equal for all A-cations with values of approximately 0.003 Å for Ru(nn) and 0.001 Å for Ru(nnn).

TABLE 3
Structural Parameters for $ACu_3Ru_4O_{12}$ Derived from XRD-Rietveld Refinements

	A	Na	Ca	Sr	Nd	La
	a (Å)	7.38489(2)	7.41871(2)	7.44754(2)	7.45780(2)	7.47800(2)
	V (Å^3)	402.747(3)	408.305(3)	413.084(3)	414.794(3)	418.173(3)
A	B_{iso}(Å^2)	0.409(18)	0.389(17)	0.554(56)	0.423(23)	0.315(22)
Cu	B_{iso}(Å^2)	0.589(18)	0.584(17)	0.632(35)	0.605(31)	0.653(29)
Ru	B_{iso}(Å^2)	0.091(8)	0.090(9)	0.293(9)	0.355(12)	0.306(12)
O	x	0.18080(55)	0.17320(60)	0.17921(75)	0.17174(64)	0.17618(65)
	y	0.30862(44)	0.30348(54)	0.30676(60)	0.29841(49)	0.30541(51)
	B_{iso}(Å^2)	0.220(53)	0.138(58)	0.001(63)	0.019(86)	0.219(80)
R_p (%)		6.30	6.93	6.55	7.69	7.11
R_{wp} (%)		8.00	8.70	8.38	9.89	9.41
R_{exp} (%)		7.03	7.57	7.22	8.64	7.73
χ^2		1.30	1.32	1.35	1.31	1.48

Note. Space group: $Im\bar{3}$ (#204). Atomic positions: A: 2a (0,0,0), Cu: 6b ($\frac{1}{2}$, 0, 0), Ru: 8c ($\frac{1}{4}$, $\frac{1}{4}$, $\frac{1}{4}$), O: 24g (x,y,0). A = Na, Ca, Sr, La, Nd.

TABLE 4
Selected Inter-Atomic Distances and Bond Angles

		Na	Ca	Sr	La	Nd
Ru–O	XRD	1.9640(13)	1.9804(15)	1.9807(18)	1.9929(16)	1.9868(16)
	EXAFS	1.9706(3)	1.9787(4)	1.9851(5)	1.9941(9)	1.9887(9)
Ru–(Cu/A)	XRD	3.19775(1)	3.21240(1)	3.22488(1)	3.23807(1)	3.22932(1)
	EXAFS	3.1930(2)	3.2137(3)	3.2193(6)	3.2363(5)	3.2300(5)
Ru–Ru(nn)	XRD	3.69245(1)	3.70936(1)	3.72377(1)	3.73900(1)	3.72890(1)
	EXAFS	3.6949(2)	3.7120(3)	3.7266(3)	3.7432(6)	3.7330(7)
Ru–Ru(nnn)	XRD	5.22191(1)	5.24582(1)	5.26621(1)	5.28774(1)	5.27346(1)
	EXAFS	5.2223(3)	5.2463(4)	5.2665(5)	5.2898(9)	5.2735(11)
Cu–O	XRD	1.9443(37)	1.9433(42)	1.9628(50)	1.9630(43)	1.9750(42)
A–O	XRD	2.6414(35)	2.5923(41)	2.6459(48)	2.6366(41)	2.5677(40)
∠Ru–O–Ru	XRD	140.1(4)	139.0(4)	140.1(5)	139.5(5)	139.6(4)
∠Cu–O–Ru	XRD	109.8(2)	109.9(2)	109.7(3)	109.2(3)	109.9(2)

This very good agreement even for large distances is noteworthy, because EXAFS is considered to be a classical short-range structural method and is usually not supposed to be well suited to derive inter-atomic distances in this range. Our results, on the other hand, prove that for appropriate samples reliable values can be achieved even for large distances.

The fact that the distances agree well although the measurements were performed at different temperatures (77 K and room temperature, respectively) further indicates that the thermal expansion coefficient of our samples must be very small. We estimate a value of approximately $2 \times 10^{-6} K^{-1}$. This is fairly in good agreement with the thermal expansion coefficient of $8 \times 10^{-6} K^{-1}$ found for the closely related compound $Cu_2Ta_4O_{12}$ (18).

Bond Valence Calculations

The expected lengths for Ru–O- and Cu–O bonds can be estimated using the bond valence (bv) approach: The total valence of a cation (V_i) is given by the sum of all the valences of its bonds $V_i = \sum_j (v_{ij})$. The commonly used empirical expression for these bond valences is $v_{ij} = \exp[(R_{ij} - d_{ij})/0.37]$ (19), where d_{ij} is the bond length and R_{ij} is the empirical bond valence parameter. Using the value of 1.834 for R_{Ru+4-O} given in Ref. (20), we obtained distances of 1.9616, 1.9840, and 2.0079 Å for $Ru^{+4.25}$, Ru^{+4}, and $Ru^{+3.75}$, respectively. In Fig. 9, a plot of the experimental bond distances vs the expected values according to the bv approach is shown. For A = Ca and Sr (i.e., Ru^{+4}) the two values agree very well. For Na, the

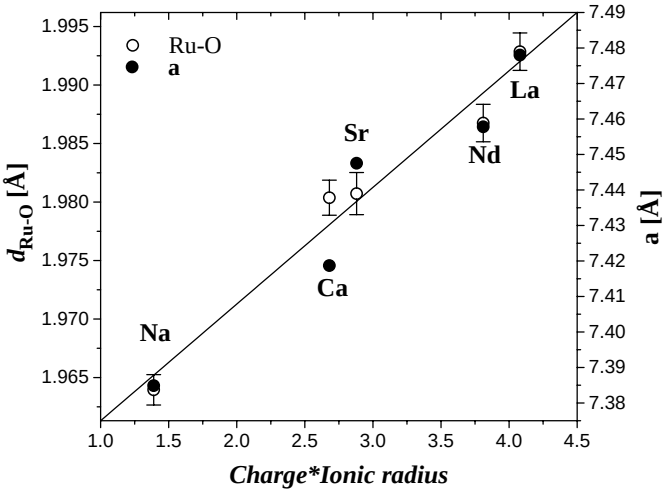

FIG. 7. Ru–O bond length and cell parameter **a** as a function of (charge ∗ ionic radius) of the A cation. Error bars for the cell parameter are too small to be seen.

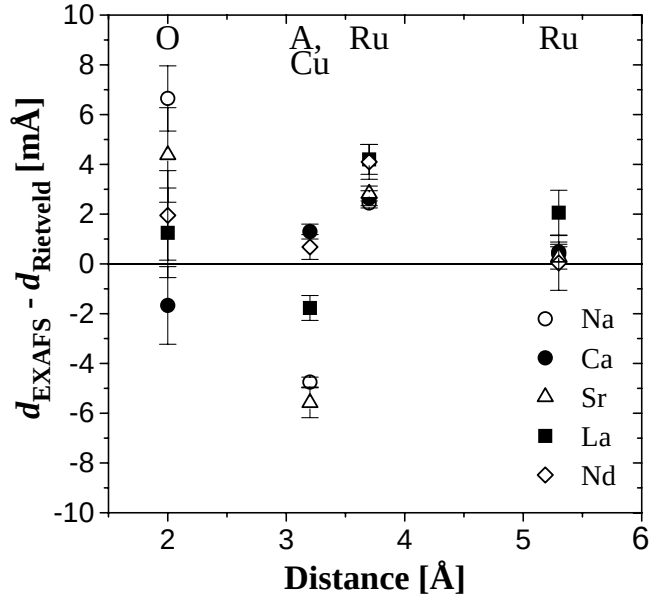

FIG. 8. Comparison between the EXAFS- and XRD-distances.

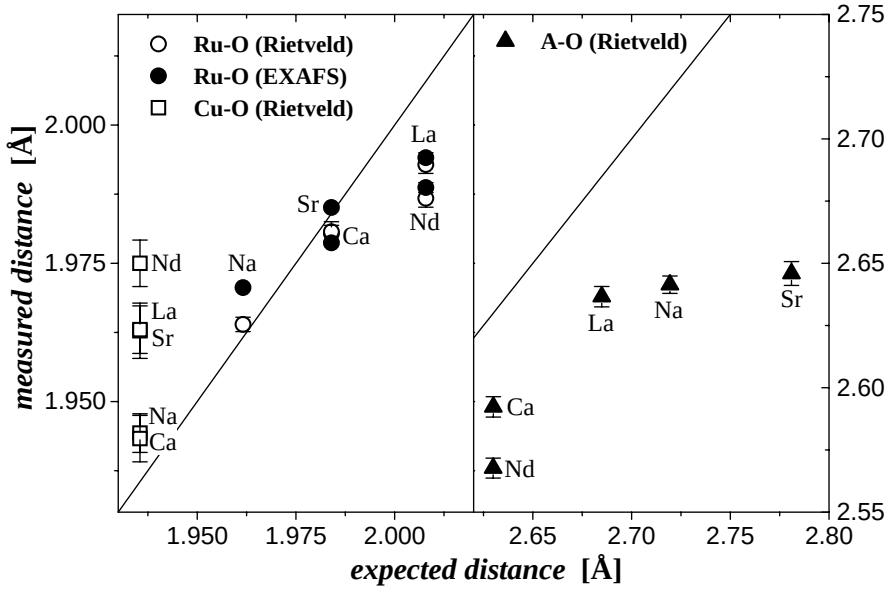

FIG. 9. Experimental inter-atomic distances vs expected values according to the bond valence theory. For copper, only the four closest oxygen neighbors are concerned. Solid lines correspond to $d_{exp} = d_{calc}$.

observed distance is equal to or slightly larger than what is expected, depending on whether the XRD- or EXAFS-value is employed. For A = La, Nd ($Ru^{+3.75}$) both XRD- and EXAFS-distances are significantly smaller than predicted by the theory. For the latter two A-cations, the experimental Ru–O distances correspond to ruthenium valence +3.90 (La) and +3.96 (Nd), respectively. We also calculated the bond valence distances for the Cu^{+2}–O bond ($R_{Cu+2-O} = 1.679$ (20)). The results are depicted in Fig. 9. While for A = Na and Ca the experimental distances for the CuO_4-square match their bv values, the distances for A = Sr, La, and Nd are too long and correspond to total copper valences of +1.86, +1.86, and +1.80, respectively. On the other hand, the bond valence of Cu is affected by the remaining eight oxygen ions belonging to the distorted cubotahedron. The four oxygens at ≈2.8 Å lead to an additional valence of approximately +0.2, while the four oxygens at ≈3.3 Å add a valence of roughly +0.05. Taking into account these contributions, the copper valences become +2.2 for Na and Ca, +2.1 for Sr and La, and +2.0 for Nd, respectively.

Even more severe deviations from the bond valence results were found for the A–O distances. The right panel of Fig. 9 shows the experimental distances (listed in Table 4) as a function of the calculated values. For all five samples the observed distances are too small, resulting in an increased valence for the A-cations of +1.24, +2.21, +2.88, +3.55, and +3.42 for Na, Ca, Sr, Nd, and La, respectively. The value for Sr is especially striking. Taking the bv calculations into account it is therefore not surprising that the Sr compound is the most difficult to prepare-with traces of $SrRuO_3$ always being present. For A = Ca, on the other hand, the deviations from the bv distances for the Ru–O, Cu–O and A–O bonds are the smallest. Consequently, this compound is very easy to prepare and single-phase samples can readily be achieved.

The bond angles Ru–O–Ru and Cu–O–Ru are listed in Table 4. It is remarkable that—although the cell parameters and bond distances change significantly—both values remain almost identical for all five compounds. The average values (and maximum deviations) are 139.7° (−0.7°) and 109.7° (−0.5°) for Ru–O–Ru and Cu–O–Ru, respectively. In addition, it is striking that the Cu–O–Ru angle is extremely close to the ideal tetrahedral angle of 109.47°. These findings are rather surprising because in perovskites, it usually changes in the tilt of the octahedra, seen through the Ru–O–Ru bond angle, which accommodate differences in size of the A site cations. In the $ACu_3Ru_4O_{12}$ family, on the other hand, we find that changes in the bond distances (especially the A–O bond) are tolerated in order to keep the metal-O-metal bond angles constant.

CONCLUSIONS

The structure of five perovskite-related oxides with the general composition $ACu_3Ru_4O_{12}$ was examined by XRD-Rietveld refinements and EXAFS spectroscopy. Additional thermogravimetric measurements revealed that the composition of all samples was very close to the idealized stoichiometry $A_1Cu_3Ru_4O_{12}$ with no vacancies at either the A- or O-sites.

For the EXAFS results, an excellent agreement between expected and observed coordination numbers was found. Apart from a few exceptions, the deviations were less than ± 0.1. An identical set of Debye–Waller factors could be used for all five samples, indicating that the thermal motion of the different atomic species is very similar in this family of compounds. The ratio of the distances Ru-(A,Cu), Ru–Ru(nn) and Ru–Ru(nnn) was found to agree very well with the ratio of 0.8660:1:1.4142 evaluated from the crystallographic symmetry.

The XRD-Rietveld refinements lead to a good agreement between the observed and calculated intensities with low R values. The displacement parameters, on the other hand, were found to be unreliably small for oxygen and in some cases also for ruthenium. In addition, the displacement parameters for Na and Ca had to be linked to the values of the Cu-ions to achieve reasonable results. Apparently, EXAFS is the better-suited method for the determination of temperature factors, at least for lighter elements like oxygen. Although the EXAFS Debye–Waller factors cannot directly be compared to the XRD values, they can be used as a rough approximation and thus provide additional information that can be useful for other methods.

A comparison of the inter-atomic distances calculated from XRD-Rietveld and Ru-K EXAFS showed very good agreements even at values up to 5 Å. This is quite surprising because EXAFS is often considered to be restricted to the direct local surrounding of the absorbing atom. Here, we were able to show that for suitable samples this method can be extended to distances even above one perovskite unit cell (≈ 4 Å).

The calculated estimated standard deviations of the inter-atomic distances should be reviewed critically. We assume that for both the XRD and EXAFS refinements a more conservative value of a few mÅ is reasonable and that both methods can lead to the same degree of accuracy.

The coordinates of all ions within the unit cell of an oxide can be calculated from their various inter-atomic distances. These can be derived from the EXAFS spectra of the different atomic species. Consequently, EXAFS and X-ray diffraction yield the same information but use a different approach: Either bond lengths are calculated from atomic positions (X-ray diffraction) or vice versa (EXAFS). In $ACu_3Ru_4O_{12}$, for example, the atomic position of the oxygen ions (x, y, 0) can be determined from the Ru–O and Cu–O distances. The corresponding Cu-K EXAFS measurements are currently in progress and results will be reported in the near future.

Bond valence calculations were carried out for the Ru–O, Cu–O and A–O bonds. For the divalent A-cations the Ru–O distances agree with the expected values. For sodium, the bond length is longer, while for A = La and Nd it is shorter than predicted by the bv theory. This means that for the latter three A-cations the Ru valence is closer to +4 than expected from the formal charge. The bond valence results for copper depend on whether only the four nearest oxygen neighbors or whether all 12 oxygens of the distorted cuboctahedron are considered: In the first case a valence of +2 is found only for A = Na and Ca, while for the other materials the effective copper valence is below +2. If all oxygens are taken into account, a valence of +2 is found for La and Nd and the effective copper valence is greater than +2 in the other three compounds studied. The A-cations are strongly effectively over-charged in all five compounds, i.e. the icosahedra around the A-cations are compressed. For A = Sr a valence of +2.88 was calculated. This severe deviation may explain why $SrCu_3Ru_4O_{12}$ is the most difficult to prepare of the set of analog samples.

The bond angles Ru–O–Ru and Cu–O–Ru, on the other hand, were found to be constant for all samples. This is surprising because generally in perovskites the BO_6-octahedra are known to rotate or tilt to adjust for different sizes of A-cations.

Our results can be discussed with respect to what has been called the "cost function" (21): Upon substitution, the crystal structure relaxes in such a way that both deviations from the preferred bond lengths are kept as low as possible and the coordination polyhedra around each atom remain as regular as possible. In the case of $ACu_3Ru_4O_{12}$, there is an additional large contribution to this cost function by the above-mentioned bond angles. Apparently, rather strong deviations from the preferred inter-atomic distances are tolerated to retain the bond angles in this family, a highly unusual situation in perovskites.

ACKNOWLEDGMENTS

Financial support by the Deutsche Forschungsgemeinschaft (SFB 484) is deeply acknowledged. Additionally, S.G.E. thanks the Deutsche Forschungsmeinschaft for a Postdoc-scholarship (Eb219-1). Thanks are due to HASYLAB for allocating beamtime and to the beamline scientists for their help.

Note added in proof. Lately, the structures of $CaCu_3Ru_4O_{12}$ and $NaCu_3Ru_4O_{12}$ were solved by single crystal X-ray diffraction (22). Cell parameters, inter-atomic distances and bond angles were found to be very similar to the results given in this work within a range of ± 0.03 Å and $\pm 1.5^\circ$, respectively.

REFERENCES

1. H. M. Rietveld, *J. Appl. Crystallogr.* **2,** 65 (1961).
2. Q. Huang, J. L. Soubeyroux, O. Chmaissem, I. Natali Sora, A. Santoro, R. J. Cava, J. J. Krajewski, and W. F. Peck Jr., *J. Solid State Chem.* **112,** 355 (1994).

3. M. K. Crawford, M. A. Subramanian, R. L. Harlow, J. A. Fernandez-Baca, Z. R. Wang, and D. C. Johnston, *Phys. Rev. B* **49,** 9198 (1994).
4. J. Mustre de Leon, *Phys. Rev. B* **44,** 4146 (1991).
5. S. Ebbinghaus, M. Fröba, and A. Reller, *J. Phys. Chem. B* **101,** 9909 (1997).
6. D. Reinen, V. Propach, *Inorg. Nucl. Chem. Lett.* **7,** 569 (1971).
7. T. Ressler, *J. Phys. IV (France)* **7,** C2-269 (1997).
8. J. J. Rehr, J. Mustre de Leon, S. I. Zabinsky and R. C. Albers, *J. Am. Chem. Soc.* **113,** 5135 (1991).
9. J. Rodríguez-Carvajal, FULLPROF: A Program for Rietveld Refinement and Pattern Matching Analysis, Abstracts of the Satellite Meeting on Powder Diffraction of the XV Congress of the IUCr, Toulouse, France, p. 127, 1990.
10. J. Muller, A. Haouzi, C. Laviron, M. Labeau, and J. C. Joubert, *Mater. Res. Bull.* **21,** 1131 (1986).
11. B. K. Teo, *J. Am. Chem. Soc.* **103,** 3990 (1981).
12. B. K. Teo, "EXAFS: Basic Principles and Data Analysis" Chapter 2, Springer, Berlin, 1986.
13. P. A. Lee, P. H. Citrin, P. Eisenberger, and B. M. Kincaid, *Rev. Mod. Phys.* **53,** 769 (1981).
14. R. D. Shannon and C. T. Prewitt, *Acta Crystallogr.* **25,** 925 (1969).
15. M. Bochu, M. N. Deschizeaux, J. C. Joubert, A. Collomb, J. Chenavas, and M. Marezio, *J. Solid State Chem.* **29,** 291 (1979).
16. Y. Ozaki, M. Ghedira, J. Chenavas, J. C. Joubert, and M. Marezio, *Acta Crystallogr. B* **33,** 3615 (1977).
17. M. Labeau, B. Bochu, J. C. Joubert, and J. Chenavas, *J. Solid State Chem.* **33,** 257 (1980).
18. J. M. Longo and A. W. Sleight, *Mater. Res. Bull.* **10,** 1273 (1975).
19. I. D. Brown and D. Altermatt, *Acta Crystallogr.* **41,** 244 (1985).
20. N. E. Brese and M. O'Keeffe, *Acta Crystallogr.* **47,** 192 (1991).
21. A. Santoro, I. Natalie Sora, and Q. Huang, *J. Solid State Chem.* **151,** 245 (2000).
22. M. A. Subramanian and A. W. Sleight, *Solid State Sciences* **4,** 347 (2002).